IEEE Access
Multidisciplinary | Rapid Review | Open Access Journal

Received September 20, 2017, accepted November 9, 2017, date of publication November 16, 2017,
date of current version December 22, 2017.

Digital Object Identifier 10.1109/ACCESS.2017.2774262

Intelligent CFAR Detector Based on Support Vector Machine

LEIOU WANG, (Member, IEEE), DONGHUI WANG, AND CHENGPENG HAO (Senior Member, IEEE)

Key Laboratory of Information Technology for Autonomous Underwater Vehicles, Chinese Academy of Sciences, Beijing 100190, China
Institute of Acoustics, Chinese Academy of Science, Beijing 100190, China

Corresponding author: Leiou Wang (wangleiou@mail.ioa.ac.cn)

This work was supported in part by the Young Talent Program of Institute of Acoustics, Chinese Academy of Science, under Grant QNYC201622, and in part by the National Natural Science Foundation of China under Grant 61571434.

ABSTRACT In this paper, we propose an intelligent constant false alarm rate detector, which uses support vector machine (SVM) techniques to improve the radar detection performance in different background environments. The proposed detector uses the variability index statistic as a feature to train a SVM and recognizes the current operational environment based on the classification results. The proposed detector has the intelligence to select the proper detector threshold adaptive to the current operational environment. This detector provides a low loss performance in homogeneous backgrounds and also performs robustly in nonhomogeneous environments including multiple targets and clutter edges.

INDEX TERMS Constant false alarm rate, support vector machine, variability index, automatic censored cell averaging, greatest of.

I. INTRODUCTION

Constant false alarm rate (CFAR) is a useful method in adaptive radar detection when the background noise is unknown. The most traditional CFAR methods are the well known mean level detectors [1]–[3]. The cell averaging (CA-) CFAR [1] has the optimal performance in a homogeneous environment for various signal-to-noise ratios (SNR). However, nonhomogeneous environments including multiple targets and clutter edges are often encountered in practice. For example, one or more interfering targets are present in the reference window for multiple targets. Moreover, clutter edges result in a transition from one level noise power to another. Unfortunately, the CA-CFAR suffers a severe performance degradation in nonhomogeneous environments. The greatest-of (GO-) CFAR [2] provides a better performance in controlling probability of false alarm (P_{fa}) in the case of clutter edges, but results in a dramatic probability of detection (P_d) loss in multiple targets. The smallest-of (SO-) CFAR [3] has better performance in multiple targets, but experiences more false alarms than the CA-CFAR in clutter edges. Moreover, the order statistics (OS-) based CFAR attempts to enhance the robustness of mean level detectors against multiple targets, but suffers from excessive false alarms in clutter edges [4]–[11]. In [12], an automatic censored cell averaging (ACCA-) CFAR detector is proposed based on an ordered data variability. The ACCA-CFAR acts like the CA-CFAR in a homogeneous environment and performs robustly in multiple targets, but experiences even more false alarms than the OS-CFAR in clutter edges. Based on above discussions, a composite detector is proposed to accommodate various environments encountered in practice. In [17], the variability index (VI-) CFAR detector is presented. The VI-CFAR dynamically switches to the CA-, SO-, or GO-CFAR, depending on the outcomes of the VI and the mean ratio (MR) hypothesis tests. However, its detection performance degrades considerably when interfering targets are not confined to a single half of the reference window [12], [17].

With machine learning achieving ground breaking success in many research fields, a switching CA/OS CFAR based on neural network (NN-CFAR) is proposed for improving the radar target detection in different environments [18]. The inputs of the neural network are the CA-CFAR threshold, the OS-CFAR threshold, and the test cell. Although the NN-CFAR is more robust in multiple targets than the CA-CFAR, its P_{fa} is even worse than the OS-CFAR during clutter edges.

Support vector machine (SVM) techniques are a powerful machine learning method for classification, regression [19] and other learning tasks [20]. In this paper, we propose an intelligent CFAR detector based on SVM (SVM-CFAR)

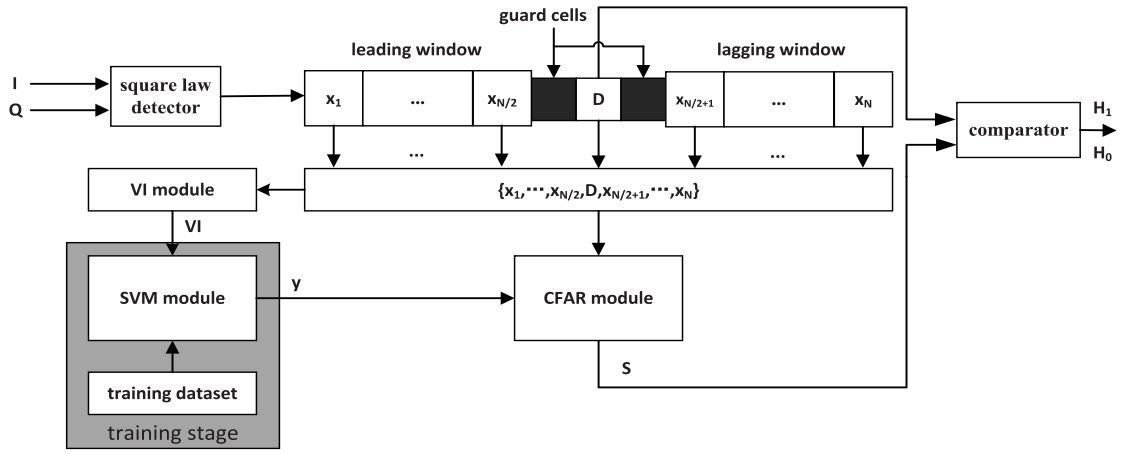

FIGURE 1. Block diagram of SVM-CFAR.

and use the VI as a feature to train the SVM. Specially, the test cell is taken into consideration to calculate the VI. The SVM-CFAR detector has the intelligence to select a proper detector threshold according to the classification results of the SVM. In this manner, the detector provides low loss performance in homogeneous backgrounds and also performs robustly in nonhomogeneous environments including multiple targets and clutter edges.

Section II discusses the operations of the SVM-CFAR including detector description, feature extraction, SVM-CFAR algorithm, and performance analysis. The SVM-CFAR simulation results for various environments are summarized in section III. Section IV gives conclusions.

II. SVM-CFAR DETECTOR

A. SVM-CFAR DETECTOR DESCRIPTION

The SVM-CFAR detector block diagram is provided in Fig. 1. In-phase I and quadrature Q input signals correspond to samples of radar range returns from a matched filter receiver. For a homogeneous noise plus clutter environment, the I and Q signals are assumed independent and identically distributed (IID) Gaussian random processes with zero mean. Consequently, the outputs of the square law detector are an exponentially distributed random variables, and are serially sent into a tapped delay line of length $N+1$. The $N+1$ samples correspond to an even number N of reference window x_n $(n = 1, 2, \cdots, N)$ and a test cell D. The reference window is divided into a leading window and a lagging window. When a target is present in the test cell, the guard cells between the reference window and the test cell prohibit target energy from invading the reference window.

For the SVM-CFAR detector, a VI module is employed to calculate the VI statistic. A *priori* data are used as a training data set. In the training stage, A SVM module is trained by using the training data set. In the practical testing stage, the SVM module outputs a decision function y based on the VI of the current reference window and the test cell. A CFAR module which contains various thresholds corresponding to different operational environments provides an adaptive threshold S according to the decision function y. For each test cell, the SVM-CFAR makes a target present or absent decision based on a comparison of the test cell to the threshold S. Precisely, A target absent decision is made if the value of the test cell is less than the threshold. Otherwise, a target present decision is made. The unique aspect of the SVM-CFAR is that it utilizes the VI as a feature to train the SVM module and provides the threshold S based on the classification results of the SVM module.

B. FEATURE EXTRACTION

The VI is a second order statistic which is function of the estimated population variance $\hat{\sigma}^2$ and estimated population mean $\hat{\mu}^2$. Specially, the test cell is taken into consideration to calculate the VI in the SVM-CFAR. In this way, we can only use the VI rather than both the VI and the MR to recognize the current operational environment.

The VI is calculated by using

$$VI = 1 + \frac{\hat{\sigma}^2}{\hat{\mu}^2} = 1 + \frac{1}{N/2+1} \sum_{i=1}^{N/2+1} \frac{(x_i - \bar{x})^2}{(\bar{x})^2}, \qquad (1)$$

where $\bar{x}$ is the arithmetic mean of the $(N/2+1)$ cells in a half reference window and test cell. The probability density function of VI will change considerably, if a target signal or interfering targets present in the test cell or the reference window and other cells only contain lower power noises.

In [17], the VI and the MR are compared with two thresholds (K_{VI} and K_{MR}) to decide that the VI and the MR come from a nonvariable or a variable environment. However, for SVM-CFAR, in the training stage, we need to predefine a nonvariable or a variable property for each training sample based on the operational environments.

A simple example of the VI in a homogeneous environment is shown in Fig. 2. The VI_A is the variability index of the leading window and test cell. The VI_B is the variability index

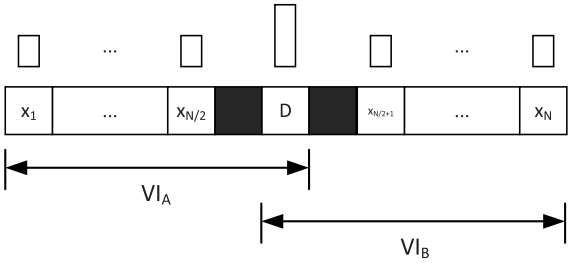

FIGURE 2. A simple example of the VI in a homogeneous environment.

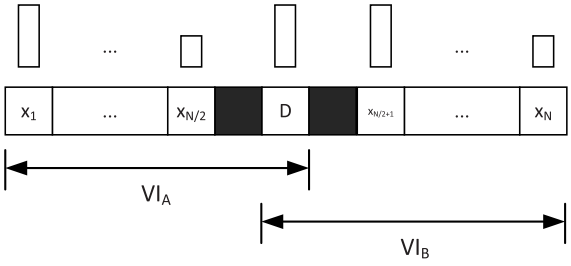

FIGURE 3. A simple example of the VI in a multiple targets environment.

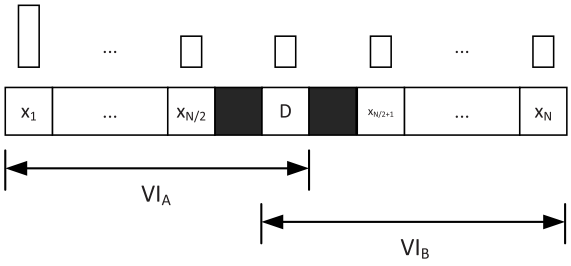

FIGURE 4. A simple example of the VI in a clutter edges environment (case a).

of the lagging window and test cell. For a homogeneous environment, a target signal is in the test cell and lower power noises are in the reference window, so we assume the VI_A and the VI_B are both variable in this situation. Similarly, if one or more interfering targets are present in the leading or lagging reference windows, the VI_A and the VI_B will still indicate a variable environment. The corresponding example is shown in Fig. 3.

For a clutter edges environment, as the clutter first enters the reference window, one or more leading window cells will occur higher power clutters. But the test cell and the lagging window only contain lower power noises. At this moment, the VI_A and the VI_B can be assumed as a variable environment and a nonvariable environment, respectively. The corresponding example is shown in Fig. 4. As the clutter continues to move into the test cell, as shown in Fig. 5, the VI_A will appear to be a nonvariable environment, but the VI_B will be a variable environment. Finally, as the clutter fills both the leading window and the lagging window, each will appear to be a nonvariable environment. The corresponding example is shown in Fig. 6.

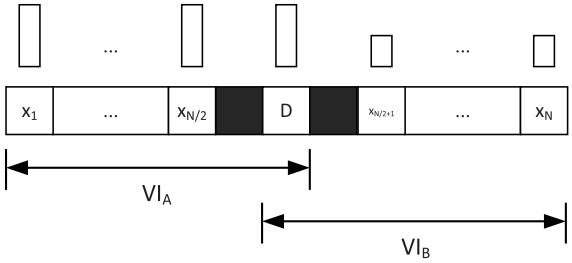

FIGURE 5. A simple example of the VI in a clutter edges environment (case b).

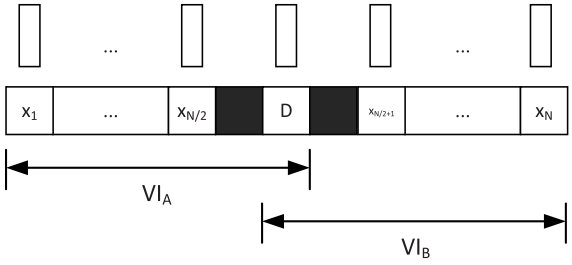

FIGURE 6. A simple example of the VI in a clutter edges environment (case c).

TABLE 1. The relationship between the VI and the operational environments.

Environment	VI_A	VI_B	Example
homogeneous	variable	variable	Fig. 2
multiple targets	variable	variable	Fig. 3
clutter edges	variable	nonvariable	Fig. 4
	nonvariable	variable	Fig. 5
	nonvariable	nonvariable	Fig. 6

In conclusion, for a homogeneous environment and multiple targets, both the VI_A and the VI_B can be assumed to be a variable environment. However, for clutter edges, either the VI_A or the VI_B appear to be a nonvariable environment. The relationship between the VI and the operational environments is shown in Table 1.

C. SVM-CFAR ALGORITHM

From above discussions, we find that the VI_A and the VI_B can be the features to classify the operational environments. On the other hand, due to the surprising classification capability, SVM is extensively used in many classified applications. SVM has two main advantages. First, in SVM, the training data are first mapped into a high dimensional feature space through a nonlinear feature mapping function. Second, SVM can find the solution of maximizing the separating margin of two different classes in this feature space while minimizing the training errors. Therefore, we consider using the VI_A and the VI_B as the features to train a SVM. Then, the SVM can output a decision function y according to the classification results.

The decision function y of the SVM module can be expressed as [21]

$$y = sgn\left(\vec{w}^T \phi\left(\vec{x}\right) + b\right), \tag{2}$$

where $\vec{x}$ is a testing sample ($\vec{x} \in R^d$, d is the dimension of the testing sample), $\vec{w}$ is a vector variable, b is a bias, T represents a transpose operator, $\phi(\vec{x})$ represents a nonlinear feature mapping function, and sgn represents a signum function [21]

$$sgn(x) = \begin{cases} -1 & if\ x < 0 \\ 0 & if\ x = 0 \\ +1 & if\ x > 0. \end{cases} \tag{3}$$

In SVM-CFAR, $\vec{x} = [VI_A, VI_B]$ (the VI_A and the VI_B comes from the current reference window and the test cell) and $d = 2$. To obtain $\vec{w}$ and b in (2), the SVM module need to be trained by using the training data set.

The distance between two different classes in the feature space is $2/\|\vec{w}\|$. To maximize the separating margin and to minimize the training errors, the primal optimization problem is

$$\begin{aligned} &\min_{\vec{w},b,\vec{\xi}} \ \frac{1}{2}\|\vec{w}\|^2 + C\sum_{i=1}^{M}\xi_i \\ &\text{subject to } y_i\left(\vec{w}^T\phi(\vec{x}_i) + b\right) \geq 1 - \xi_i, \\ &\qquad \xi_i \geq 0, \quad i = 1, 2, \cdots, M, \end{aligned} \tag{4}$$

where $\vec{x}_i$ is ith training sample, y_i is the corresponding label ($y_i \in \{-1, 1\}$ for a two-classes pattern), $(\vec{x}_i, y_i)$ represents ith training data, ξ_i is the training error of ith training data, M is the number of the training data, and C is the regularization parameter which provides a tradeoff between the distance of the separating margin and the training errors. In SVM-CFAR, $\vec{x}_i = \left[VI_{A,i}, VI_{B,i}\right]$, where $VI_{A,i}$ and $VI_{B,i}$ are the VI_A and VI_B of ith training sample, respectively. Moreover, based on the discussions in Table 1, if the operational environment of ith training sample is clutter edges, we will define $y_i = -1$. Otherwise, $y_i = 1$.

Due to the possible high dimensionality of the vector variable $\vec{w}$, (4) is equivalent to solving the following dual problem [21]

$$\begin{aligned} &\min_{\vec{\alpha}} \ \frac{1}{2}\sum_{i=1}^{M}\sum_{j=1}^{M} y_i y_j \alpha_i \alpha_j \phi(\vec{x}_i)^T \phi\left(\vec{x}_j\right) - \sum_{i=1}^{M}\alpha_i \\ &\text{subject to } \sum_{i=1}^{M} y_i \alpha_i = 0, \\ &\qquad 0 \leq \alpha_i \leq C, \quad i = 1, 2, \cdots, M, \end{aligned} \tag{5}$$

where each Lagrange multiplier α_i corresponds to ith training data $(\vec{x}_i, y_i)$. The kernel function $K\left(\vec{x}_i, \vec{x}_j\right) = \phi(\vec{x}_i)^T\phi\left(\vec{x}_j\right)$, so we have

$$\begin{aligned} &\min_{\vec{\alpha}} \ \frac{1}{2}\sum_{i=1}^{M}\sum_{j=1}^{M} y_i y_j \alpha_i \alpha_j K\left(\vec{x}_i, \vec{x}_j\right) - \sum_{i=1}^{M}\alpha_i \\ &\text{subject to } \sum_{i=1}^{M} y_i \alpha_i = 0, \\ &\qquad 0 \leq \alpha_i \leq C, \quad i = 1, 2, \cdots, M. \end{aligned} \tag{6}$$

TABLE 2. The adaptive threshold S of the SVM-CFAR in different environments.

Environment	Decision Function y	Adaptive Threshold
homogeneous multiple targets	$y = 1$	$S = S_{ACCA}$
clutter edges	$y = -1$	$S = S_{GO}$

After (6) is solved, using the primal-dual relationship, the optimal $\vec{w}$ satisfies

$$\vec{w} = \sum_{i=1}^{M_s} y_i \alpha_i \phi(\vec{x}_i), \tag{7}$$

where M_s is the number of support vectors. The decision function y of the SVM module can be rewritten as

$$y = sgn\left(\sum_{i=1}^{M_s} y_i \alpha_i K(\vec{x}_i, \vec{x}) + b\right). \tag{8}$$

In (8), α_i and b can be obtained through the training stage. Then, to get the decision function y, we only need to substitute the $\vec{x}$ into (8) in the practical test stage.

In general, the radial basis function (RBF) kernel is a reasonable first choice [22]

$$RBF: K\left(\vec{x}_i, \vec{x}_j\right) = exp\left(-\sigma\left\|\vec{x}_i - \vec{x}_j\right\|^2\right), \quad \sigma > 0, \tag{9}$$

where σ is kernel parameters, and exp represents an exponent function.

The SVM module consumes extra computational costs. However, there are many methods to alleviate the extra computational costs in the SVM-CFAR. First, the most computational tasks are completed during the training stage. Second, only the support vectors can participate in the computation of (8). The last but most important method is that using the VI rather than the entire reference window [19] as a feature to train the SVM module can dramatically reduce the computational burdens. This is because the computational costs of a SVM is order (exp^d) [21], [22]. Fortunately, d of the SVM-CFAR is merely 2 through feature extraction.

D. THE CFAR MODULE

The CFAR module of the SVM-CFAR contains two CFAR detectors, the ACCA-CFAR and the GO-CFAR. The CFAR module calculates one adaptive threshold S from the two detectors according to the decision function y. $y = 1$ indicates that the current operational environment is a homogeneous environment or multiple targets, so $S = S_{ACCA}$ (S_{ACCA} is the adaptive threshold of ACCA-CFAR). On the contrary, $y = -1$ indicates that the current operational environment is clutter edges, so $S = S_{GO}$ (S_{GO} is the adaptive threshold of GO-CFAR). The adaptive threshold S of the SVM-CFAR in different environments is shown in Table 2.

TABLE 3. The training data set in our simulations.

Environments	Position of Interfering Targetor or Clutter Edges	Target SNR (dB)	Training Sample Number	Label
homogeneous	-	0	10	
		3	10	
		⋮	⋮	
		30	10	
	x_1	0	10	
		3	10	
		⋮	⋮	
		30	10	
multiple targets	x_2	0	10	
		3	10	1
		⋮	⋮	
		30	10	
	⋮	⋮	⋮	
	x_N	0	10	
		3	10	
		⋮	⋮	
		30	10	
clutter edges	-	0	10	
		3	10	
		⋮	⋮	
		30	10	
	x_1	0	10	
		3	10	
		⋮	⋮	
		30	10	
	x_2	0	10	
		3	10	-1
		⋮	⋮	
		30	10	
	⋮	⋮	⋮	
	x_N	0	10	
		3	10	
		⋮	⋮	
		30	10	

E. SVM-CFAR PERFORMANCE ANALYSIS

The goal of the SVM-CFAR is to achieve a good performance in different environments, which requires that the SVM module has a low probability of classification error. Based on above discussions, $y = 1$ and $D > S_{ACCA}$ indicate that the current operational environment is a homogeneous environment or multiple targets and there is a target in the test cell. However, if the SVM module outputs $y = -1$ due to classification error and $D < S_{GO}$, this classification error will degrade the P_d of the SVM-CFAR. A P_d hypothesis test for a two-classes pattern is defined as

$$\beta = P\left[y = -1, D < S_{GO} \,|y = 1, D > S_{ACCA}\right]. \quad (10)$$

From (10), we can find that a classification error may increase β. The relationship between the P_d of the SVM-CFAR and β can be expressed as

$$P_{d,svm} = P_{d,desired} - \beta, \quad (11)$$

where $P_{d,desired}$ is a desired P_d, which corresponds to the P_d of the ACCA-CFAR for homogeneous environments and multiple targets. From (11), it can be seen that the greater β, the worse $P_{d,svm}$.

In an analogous fashion, $y = -1$ and $D < S_{GO}$ indicate that the current operational environment is clutter edges and there is no target in the test cell. However, if the SVM module

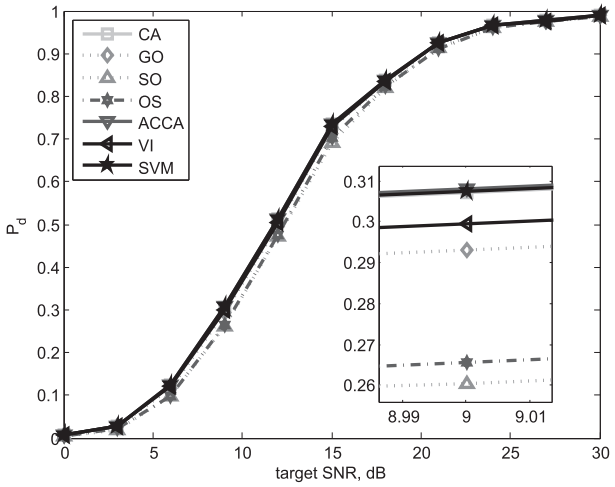

FIGURE 7. P_d against SNR of CA-CFAR, GO-CFAR, SO-CFAR, OS-CFAR, ACCA-CFAR, VI-CFAR, and SVM-CFAR in homogeneous environments.

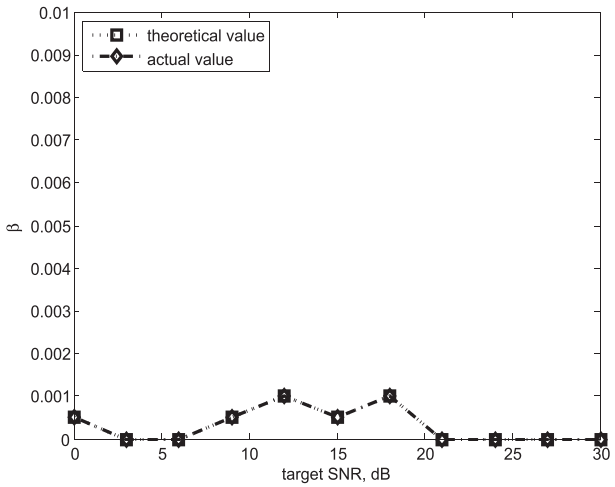

FIGURE 8. β in homogeneous environments.

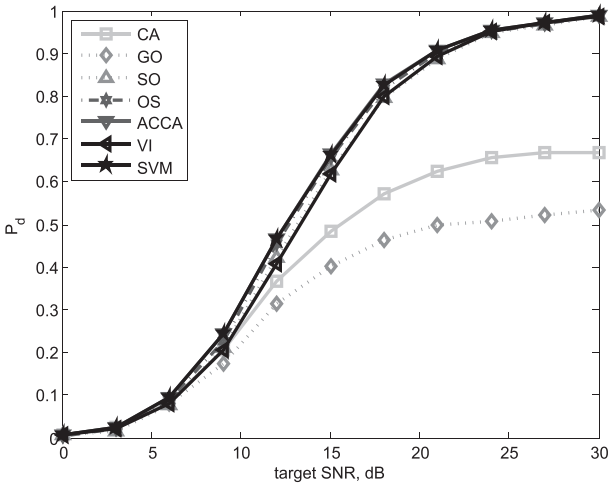

FIGURE 9. P_d against SNR of CA-CFAR, GO-CFAR, SO-CFAR, OS-CFAR, ACCA-CFAR, VI-CFAR, and SVM-CFAR in one interfering target environments.

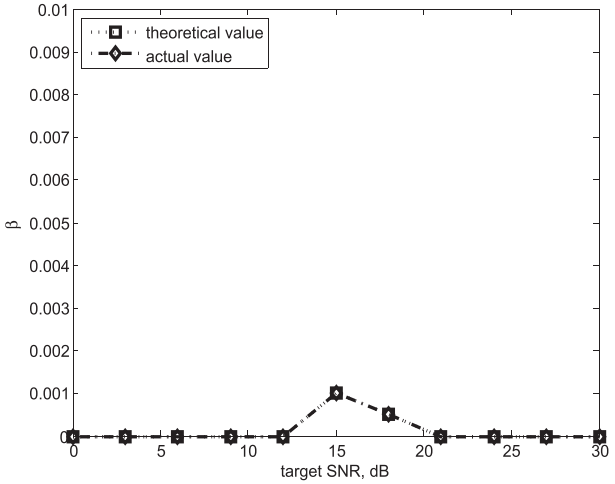

FIGURE 10. β in one interfering target environments.

outputs $y = 1$ due to classification error and $D > S_{ACCA}$, this classification error will degrade the P_{fa} of the SVM-CFAR. A P_{fa} hypothesis test for a two-classes pattern is defined as

$$\gamma = P\left[y = 1, D > S_{ACCA} \,|y = -1, D < S_{GO}\right]. \quad (12)$$

Similarly, from (12), we can find that a classification error may increase γ. The relationship between the P_{fa} of the SVM-CFAR and γ can be expressed as

$$P_{fa,svm} = P_{fa,desired} + \gamma, \quad (13)$$

where $P_{fa,desired}$ is a desired P_{fa}, which corresponds to the P_{fa} of the GO-CFAR for clutter edges. From (13), it can be seen that the greater γ, the worse $P_{fa,svm}$.

III. PERFORMANCE OF SVM-CFAR DETECTOR

A. TRAINING DATA SET

For a design $P_{fa} = 10^{-4}$, we study the performance of the SVM-CFAR for $N = 24$. The training data set in our simulations is shown in Table 3. The notation – and ⋮ represent none and ellipsis, respectively. The multiple targets contain one interfering target in different positions of the reference window. The clutter enters the reference window from x_1 to x_N for clutter edges. The target SNR $= [0, 3, 6, 9, 12, 15, 18, 21, 24, 27, 30]$ (dB). Therefore, the total number of the training data set $M = 2{*}25{*}11{*}10 = 5500$. The SVM module is implemented by using the LIBSVM library [22]. In our simulations, we choose the *RBF* kennel function with $C = 1$ and $\sigma = 1$ through a grid-search method [22]. $M_s = 2662$.

The detection performance of the well trained SVM-CFAR is compared to those of the CA-CFAR, the GO-CFAR, the SO-CFAR, the OS-CFAR, the ACCA-CFAR, and the VI-CFAR detectors in different environments. The censoring point of the OS-CFAR is $3N/4$ [5], [7]. For the ACCA-CFAR, we take the lowest cell $p = 16$ [12].

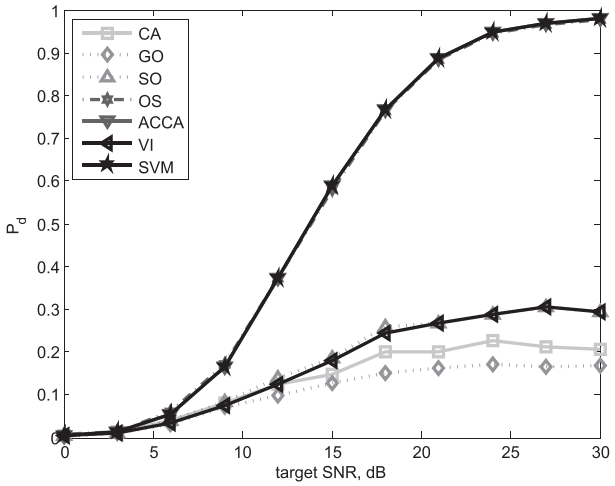

FIGURE 11. P_d against SNR of CA-CFAR, GO-CFAR, SO-CFAR, OS-CFAR, ACCA-CFAR, VI-CFAR, and SVM-CFAR in four interfering targets environments.

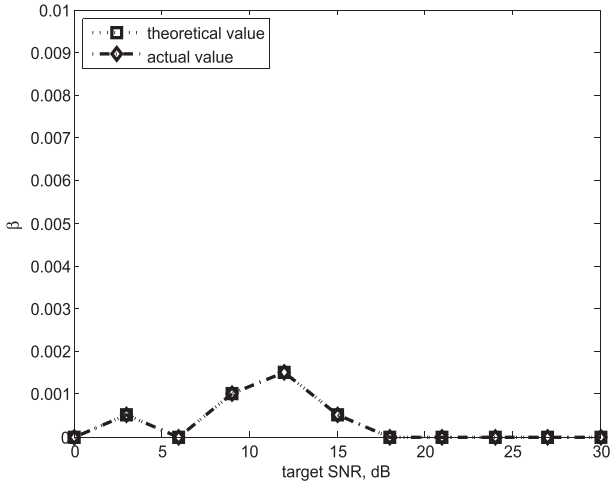

FIGURE 12. β in four interfering targets environments.

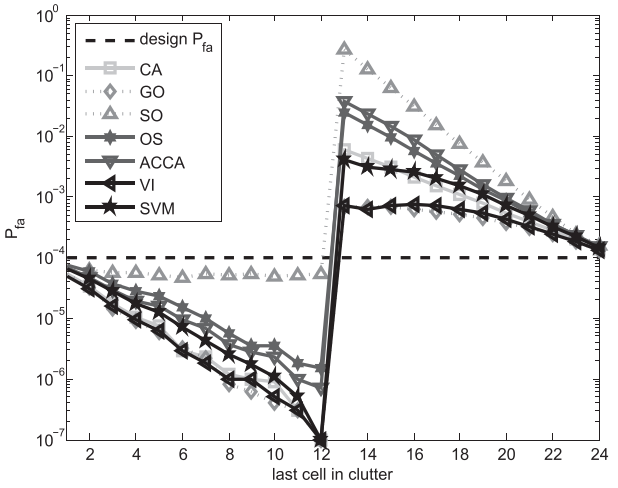

FIGURE 13. P_{fa} of CA-CFAR, GO-CFAR, SO-CFAR, OS-CFAR, ACCA-CFAR, VI-CFAR, and SVM-CFAR in clutter edges environments.

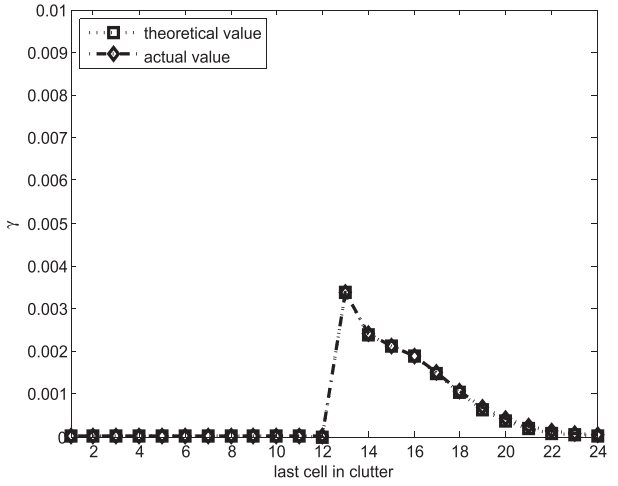

FIGURE 14. γ in clutter edges environments.

B. SIMULATION RESULTS

In Fig. 7, we present the P_d of these detectors in a homogeneous backgrounds. We observe that the SVM-CFAR acts like the CA-CFAR and the ACCA-CFAR in homogeneous backgrounds. The SVM-CFAR detector slightly performs better than the VI-CFAR and the GO-CFAR, and is obviously superior to the OS-CFAR and the SO-CFAR. Fig. 8 shows β, which is less than 0.001 for different target SNRs in the test cell. The actual value of β agrees very well with theoretical value which is calculated by using (11).

Fig. 9 shows that the P_d in the environments with a single interfering target. We can find that the CA-CFAR and the GO-CFAR have a substantial performance degradation while the performance of the SVM-CFAR, the OS-CFAR, and the ACCA-CFAR is relatively unaffected. The SVM-CFAR performance is somewhat better relative to the SO-CFAR and the VI-CFAR. Like the ACCA-CFAR, the SVM-CFAR detector is not affected by the position of the interfering target in the reference window. Fig. 11 shows that P_d for the case of four interfering targets both in the leading window and the lagging window. In this case, the detection performance degradation of the SO-CFAR and the VI-CFAR is more severe. We note that the SVM-CFAR and the ACCA-CFAR are robust in the sense that no excessive detection degradation occurs. Fig. 10 and Fig. 12 show the β for one interfering target and four interfering targets, respectively. We observe that β is still very small for these cases.

The P_{fa} of the SVM-CFAR in clutter edges environments is shown in Fig. 13 where the clutter-to-noise ratio (CNR) is 10dB. We observe that the P_{fa} of the SVM-CFAR ($P_{fa,svm} \approx 0.004$) is somewhat worse relative to the P_{fa} of the GO-CFAR ($P_{fa,go} \approx 0.0006$) and the P_{fa} of the VI-CFAR ($P_{fa,vi} \approx 0.0007$) when the clutter transition occurs at the test cell. This is because when the clutter fills the test cell, there is a relatively greater γ (although the maximum of γ is less than 0.0034), as shown in Fig. 14. However, the P_{fa} of the SVM-CFAR is somewhat better relative to the P_{fa} of

the CA-CFAR ($P_{fa,ca} \approx 0.0061$) and far better than the P_{fa} of the OS-CFAR ($P_{fa,os} \approx 0.0252$), the P_{fa} of the ACCA-CFAR ($P_{fa,acca} \approx 0.0378$), and the P_{fa} of the SO-CFAR ($P_{fa,so} \approx 0.2673$).

IV. CONCLUSION

An intelligent CFAR detector based on support vector machine techniques is proposed. The proposed detector uses the variability index as the feature to train a SVM module and can select the proper threshold according to the classification results of the SVM module for different environments. The simulation results show that the proposed detector provides low loss performance in homogeneous backgrounds and also performs robustly in nonhomogeneous environments including multiple targets and clutter edges. Moreover, many researchers have studied the properties of non-Gaussian distributions in recent years, such as Weibull distribution, K distribution, Pareto distribution, and so on. Therefore, we consider using machine learning techniques to improve the detection performance for above distributions in future work.

ACKNOWLEDGEMENTS

The authors are grateful to the anonymous reviewers for their constructive comments.

REFERENCES

[1] H. M. Finn and R. S. Johnson, "Adaptive detection mode with threshold control as a function of spatially sampled clutter estimates," *RCA Rev.*, vol. 29, no. 3, pp. 414–464, 1968.
[2] V. Hansen and J. Sawyers, "Detectability loss due to 'greatest of' selection in a cell-averaging CFAR," *IEEE Trans. Aerosp. Electron. Syst.*, vol. AES-16, no. 1, pp. 115–118, Jan. 1980.
[3] G. V. Trunk, "Range resolution of targets using automatic detectors," *IEEE Trans. Aerosp. Electron. Syst.*, vol. AES-14, no. 5, pp. 750–755, Sep. 1978.
[4] J. T. Rickard and G. M. Dillard, "Adaptive detection algorithms for multiple-target situations," *IEEE Trans. Aerosp. Electron. Syst.*, vol. AES-13, no. 4, pp. 338–343, Jul. 1977.
[5] H. Rohling, "Radar CFAR thresholding in clutter and multiple target situations," *IEEE Trans. Aerosp. Electron. Syst.*, vol. AES-19, no. 4, pp. 608–621, Jul. 1983.
[6] P. P. Gandhi and S. A. Kassam, "Analysis of CFAR processors in homogeneous background," *IEEE Trans. Aerosp. Electron. Syst.*, vol. AES-24, no. 4, pp. 427–445, Jul. 1988.
[7] J. A. Ritcey and J. L. Hines, "Performance of MAX family of order-statistic CFAR detectors," *IEEE Trans. Aerosp. Electron. Syst.*, vol. 27, no. 1, pp. 48–57, Jan. 1991.
[8] M. B. El Mashade, "Detection analysis of linearly combined order statistic CFAR algorithms in nonhomogeneous background environments," *Signal Process.*, vol. 68, no. 1, pp. 59–71, 1998.
[9] C.-J. Kim, H.-S. Lee, and D.-S. Han, "Generalized OS CFAR detector with noncoherent integration," *Signal Process.*, vol. 31, no. 1, pp. 43–56, 1993.
[10] S. D. Himonas and M. Barkat, "Automatic censored CFAR detection for nonhomogeneous environments," *IEEE Trans. Aerosp. Electron. Syst.*, vol. 28, no. 1, pp. 286–304, Jan. 1992.
[11] R. Srinivasan, "Robust radar detection using ensemble CFAR processing," *IEE Proc.-Radar, Sonar Navigat.*, vol. 147, no. 6, pp. 291–297, Dec. 2000.
[12] A. Farrouki and M. Barkat, "Automatic censoring CFAR detector based on ordered data variability for nonhomogeneous environments," *IEE Proc.-Radar, Sonar Navigat.*, vol. 152, no. 1, pp. 43–51, Feb. 2005.
[13] X. Meng, "Performance analysis of Nitzberg's clutter map for Weibull distribution," *Digit. Signal Process.*, vol. 20, no. 3, pp. 916–922, 2010.
[14] X. W. Meng, "Performance analysis of OS-CFAR with binary integration for weibull background," *IEEE Trans. Aerosp. Electron. Syst.*, vol. 49, no. 2, pp. 1357–1366, Apr. 2013.
[15] C. Y. Chong, F. Pascal, J.-P. Ovarlez, and M. Lesturgie, "MIMO radar detection in non-Gaussian and heterogeneous clutter," *IEEE J. Sel. Topics Signal Process.*, vol. 4, no. 1, pp. 115–126, Feb. 2010.
[16] T. Jian, Y. He, F. Su, C. Qu, and D. Ping, "Adaptive detection of sparsely distributed target in non-Gaussian clutter," *IET Radar, Sonar Navigat.*, vol. 5, no. 7, pp. 780–787, Aug. 2011.
[17] M. E. Smith and P. K. Varshney, "Intelligent CFAR processor based on data variability," *IEEE Trans. Aerosp. Electron. Syst.*, vol. 36, no. 3, pp. 837–847, Jul. 2000.
[18] B. P. A. Rohman, D. Kurniawan, and M. T. Miftahushudur, "Switching CA/OS CFAR using neural network for radar target detection in non-homogeneous environment," in *Proc. Int. Electron. Symp.*, Sep. 2015, pp. 280–283.
[19] J. E. Ball, "Low signal-to-noise ratio radar target detection using linear support vector machines (L-SVM)," in *Proc. IEEE Rader Conf.*, May 2014, pp. 1291–1294.
[20] D. He and H. Leung, "CFAR intrusion detection method based on support vector machine prediction," in *Proc. IEEE Int. Conf. Comput. Intell. Meas. Syst. Appl.*, Jul. 2004, pp. 10–15.
[21] C. Cortes and V. N. Vapnik, "Support vector networks," *Mach. Learn.*, vol. 20, no. 3, pp. 273–297, 1997.
[22] C.-C. Chang and C.-J. Lin, "LIBSVM: A library for support vector machines," *ACM Trans. Intell. Syst. Technol.*, vol. 2, no. 3, p. 27, 2011. [Online]. Available: http://www.csie.ntu.edu.tw/~cjlin/libsvm

LEIOU WANG (M'16) received the B.S. degree in communication engineering and the M.S. degree in computer application technology from Beijing Union University, Beijing, China, in 2007 and 2011, respectively, and the Ph.D. degree in signal and information processing from the University of Chinese Academy of Sciences, Beijing, in 2015. He is currently an Assistant Professor with the Key Laboratory of Information Technology for Autonomous Underwater Vehicles, Chinese Academy of Sciences. His research interests include statistical signal processing with more emphasis on adaptive radar signal processing, and circuits and systems low power technology.

DONGHUI WANG received the B.S. degree from Tsinghua University, Beijing, China, in 1997, and the Ph.D. degree in microelectronics and solid state electronics from the Institute of Semiconductors, Chinese Academy of Sciences, Beijing, in 2002. He is currently a Professor with the Key Laboratory of Information Technology for Autonomous Underwater Vehicles, Chinese Academy of Sciences. His research interests are VLSI design and DSP processor design.

CHENGPENG HAO (M'08–SM'15) received the B.S. and M.S. degrees in electronic engineering from the Communication University of China, Beijing, China, in 1998 and 2001, respectively, the Ph.D. degree in signal and information processing from the Institute of Acoustics, Chinese Academy of Sciences, Beijing, in 2004. He has held a visiting position with the Electrical and Computer Engineering Department, Queen's University, Kingston, Canada, from 2013 to 2014. He is currently a Professor with the Key Laboratory of Information Technology for Autonomous Underwater Vehicles, Chinese Academy of Sciences. His research interests include statistical signal processing with more emphasis on adaptive sonar and radar signal processing.